

# Unbalanced Cylindrical Magnetron for Accelerating Cavities Coating

G. Rosaz, V. Semblanet, S. Calatroni, A. Sublet, M. Taborelli

**Abstract**—We report in this paper the design and qualification of a cylindrical unbalanced magnetron source. The dedicated magnetic assemblies were simulated using a finite element model. A hall-effect magnetic probe was then used to characterize those assemblies and compared to the theoretical magnetic profiles. These show a good agreement between the expected and actual values. The qualification of the different magnetic assemblies was then performed by measuring the ion flux density reaching the surface of the sample to be coated using a commercial retarding field energy analyzer. The strongest unbalanced configuration shows an increase from  $0.016 \text{ A.cm}^{-2}$  to  $0.074 \text{ A.cm}^{-2}$  of the ion flux density reaching the sample surface compared to the standard balanced configuration for a pressure  $5.10^{-3}$  mbar and a plasma source power of 300 W.

**Keywords**—Ion energy distribution, niobium, retarding field energy analyzer, sputtering, SRF cavity, unbalanced magnetron.

## I. INTRODUCTION

**S**UPERCONDUCTING radiofrequency (SRF) accelerating cavities are used to propel particles in accelerators such as the Large Hadron Collider (LHC). The technology that has been chosen for the latter is to use copper cavities that are coated with a thin layer of niobium deposited by DC magnetron sputtering. The advantage of this technological choice is to prevent the risk of quenching the cavities thanks to the high thermal conductivity of copper. Furthermore, the use of a thin film of niobium and a cheap substrate material such as copper reduces significantly the cost of fabrication compared to bulk niobium cavities. Finally copper based cavities are not sensitive to earth magnetic field and thus do not need any magnetic shielding for operation that reduces even more the cost of the final apparatus. Despite these advantages, numerous problems remain to be tackled in order to get the Nb/Cu technology competitive with the performance of bulk niobium. One of those is the dependence of the film superconducting properties on the impinging angle of the sputtered atoms on the cavity surface. This effect has been seen in SRF cavities [1] as well as on samples [2].

We have shown a similar effect by coating samples tilted at different angles with respect to the niobium target used in our coating setup. Scanning electron microscopy (SEM) investigations have pointed out a strong portion of voids in the layers that is increasing when tilting the samples (Fig.1) which suggest a variation of the layer quality in the different regions of the SRF cavities.

G. Rosaz, S. Calatroni, V. Semblanet, A. Sublet and M. Taborelli are with CERN TE-VSC, CH-1211 Geneva, Switzerland (e-mail: guillaume.rosaz@cern.ch).

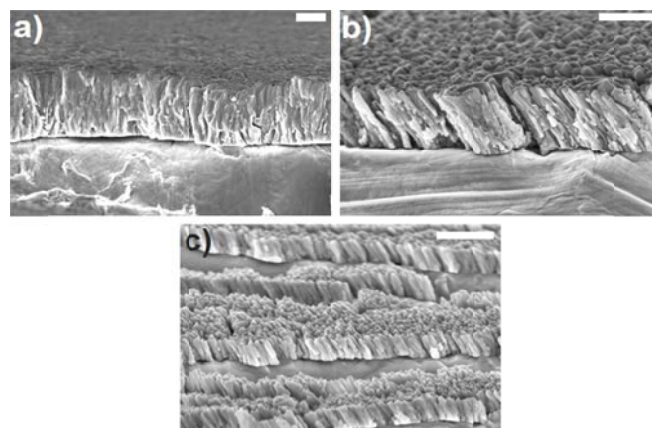


Fig. 1 SEM Cross sections of Nb films deposited by magnetron sputtering at various tilted angle of (a)  $0^\circ$ , (b)  $45^\circ$  and (c)  $90^\circ$ : Scale bars all represent a 400 nm length.

Reducing the porosity would help improving the superconducting properties and thus lead to better performances of the SRF cavities. In order to densify the Nb layer, we studied a design of unbalanced magnetron. Such a configuration is indeed known to enable more ions from the plasma to reach the sample surface and hence to enhance the thin film density by ion bombardment [3], [4].

In the following, we present the coating apparatus that is used to coat SRF cavities and we point out the technical challenges of such a geometry. Furthermore, we propose magnetic configurations with different unbalancing degrees and characterize the associated surface ion flux density.

## II. EXPERIMENTAL SETUP

The coating setup used for this study is described in Fig. 2. Krypton is used as the sputtering gas. Total pressure in the cavity is controlled with a capacitance gauge and is comprised between  $1.10^{-3}$  mbar and  $1.10^{-2}$  mbar.

The cavity, which is also used as the vacuum chamber, is 413 mm in length and 200 mm wide at the equator of the cell. It is electrically insulated from ground and thus its potential can be controlled. Along this study however, it has been kept at the reference ground potential. A Huttinger Truplasma 3005 power supply is used for the DC plasma generation. The total power used in this study ranges between 50W and 300W.

The position of the plasma can be tuned by moving the magnet inside the tubular Nb cathode.

A retarding field energy analyzer (RFA) from Impedans is mounted on the cavity at the equator position in order to measure the ion flux density at its surface.

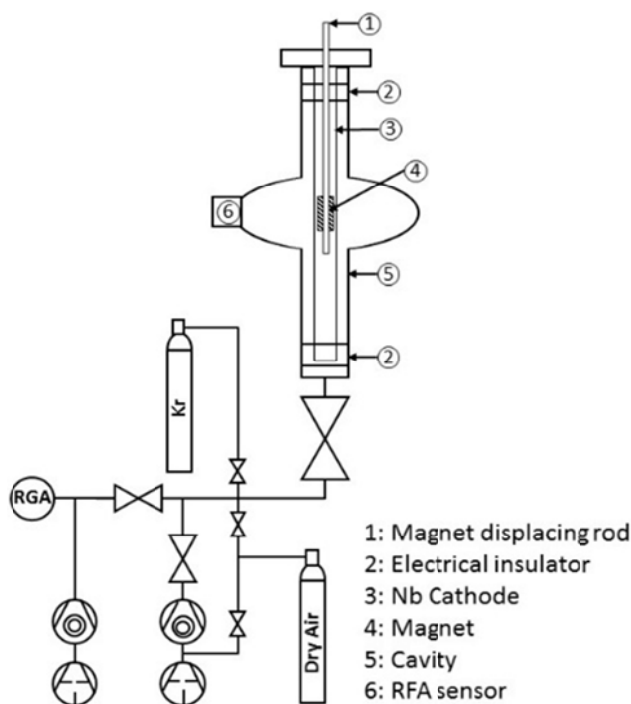


Fig. 2 Schematic of the SRF cavities coating apparatus

### III. OBJECTIVES

The standard magnet used to perform the sputtering of niobium is a cylinder of internal diameter 10.3 mm, external diameter 30 mm and 50 mm in length. It is made of SmCo with a remanent magnetization of approximately 1.1 T and a coercive field of 760 kA.m<sup>-1</sup>. The magnetization is aligned parallel to the cylinder axis.

Finite element simulations carried out using Femm42 show that this type of magnetic configuration belongs to the so-called balanced magnetron.

The goal of this study is to propose a new magnetic assembly that could increase the ion flux density at the surface of the cavity to enhance the ionic assistance during the coating. To do so we have to take into account some limitations of the system. First of all the cooling of the cathode is done by flowing compressed air in the volume surrounding the magnet. This fact determines the type material that can be used for the magnet which is necessarily SmCo. Compared to NdFeB magnets SmCo can withstand much higher working temperature while developing strong magnetic field (~1T) that is needed to ensure a proper electron confinement in the discharge at the surface of the cathode.

The size of the magnets cannot be bigger than 30mm in diameter in order to fit inside the tubular cathode. Finally, for a much more convenient assembly we decided to use cylindrical magnets that are necessarily magnetized along the cylinder axis. It is thus necessary to combine this geometry with poles made of a material with strong magnetic permeability in order to redirect the magnetic flux perpendicular to the cathode surface, thus ensuring an efficient confinement of the plasma electrons (see Fig. 3).

TABLE I  
MAGNET AND POLES' MAGNETIC PROPERTIES

| Quantity                            | Magnet     | External Poles | Internal Pole |
|-------------------------------------|------------|----------------|---------------|
| Length (mm)                         | 12         | 2              | 36            |
| Internal diameter (mm)              | 10.3       | 10.3           | 10.3          |
| External diameter (mm)              | 28         | 30             | 28            |
| Material                            | SmCo       | Fe (99.99%)    | Fe(99.99%)    |
| Remanence (T)                       | 1.1        | -              | -             |
| Coercive Field (A.m <sup>-1</sup> ) | 760000 ±48 | 60-120         | 60-120        |
| Permeability                        | 1.05       | 3500-6000      | 3500-6000     |

### IV. MAGNETIC ASSEMBLIES

Finite element simulations have been carried out using the Femm42 software [5] in order to propose two new configurations belonging to the unbalanced magnetron scheme and to compare them with the original magnet. Their unbalancing degree can be expressed by (1) according to [6]

$$K_G = \frac{R_0}{2L} \quad (1)$$

where L is the average length of the cathode eroded area (in our case 30 mm) and R<sub>0</sub> is the distance from the target surface to the point on the axis of the magnetron where the normal component of the magnetic field (B<sub>z</sub>) has a value of zero.

Two unbalanced configurations have been identified. Both are obtained by combining multiple magnets in order to tune the strength of the external poles with respect to the central pole. The suitable magnets and iron poles characteristics have then been defined and are summarized in Table I. The K<sub>G</sub> factors of the different configurations are summarized in Table II. A schematic of these assemblies is presented in Fig. 3 with the associated field lines distribution.

TABLE II  
SUMMARY OF THE DIFFERENT MAGNETIC CONFIGURATIONS PROPERTIES

| Configuration | K <sub>G</sub> factor |
|---------------|-----------------------|
| Balanced      | 3.31                  |
| Unbalanced 1  | 3.01                  |
| Unbalanced 2  | 1.46                  |

The magnetic profiles of both the tangential and normal component of the magnetic field with respect to the surface of the magnetic assembly have been simulated and experimentally validated by measuring them using a Hall-effect magnetic probe.

Fig. 4 depicts the theoretical and experimental values of the magnetic field developed at the magnet surface by the Unbalanced 2 configuration.

Both predicted and actual values appear to be in good agreement despite few discrepancies that can be attributed to the measurement spatial accuracy. One can also notice a slightly asymmetric behavior of the normal component that may be related to non-uniformity of the magnets. These results still validate our theoretical predictions and comfort us in predicting our magnetic profiles using finite element simulations. All the magnetic assemblies were characterized in the same way (graphs not shown) and exhibited a similar agreement between theoretical and experimental values. The

effect of each of these magnetic assemblies was then characterized using a retarding field energy analyzer.

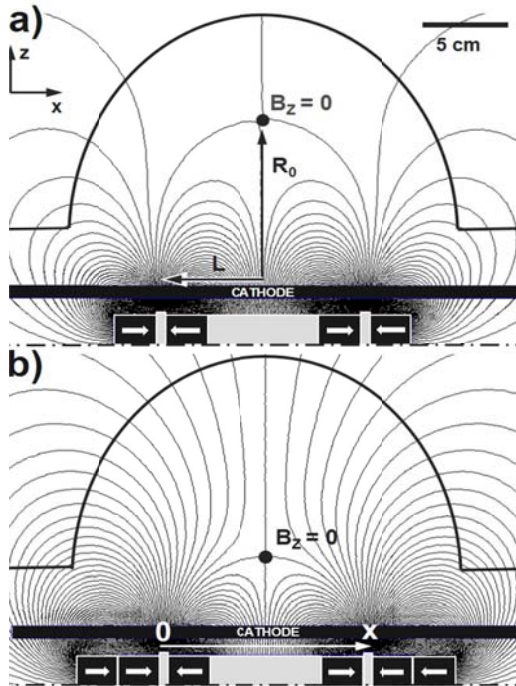


Fig. 3 Schematic of the two unbalanced magnetic configurations: Only one slice having rotational symmetry around the cavity axis is represented. The dark squares are the SmCo magnets and light grey ones are the iron poles. The arrows show the magnetization orientation (a) unbalanced 1 and (b) unbalanced 2: The cavity is depicted in continuous black line, its axis as dash-dotted lines

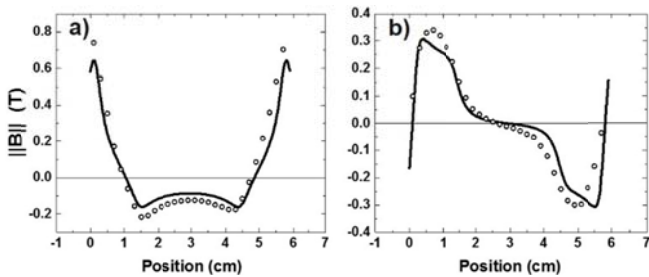


Fig. 4 Experimental (open dots) and theoretical (lines) values of the a) normal and b) tangential component of the magnetic field at the magnet surface of the unbalanced 2 configuration

## V. ION FLUX DENSITIES MEASUREMENTS

### A. Semion Sensor

The SEMiON RFA sensor contains four different grids. The first one acts as a geometrical filter in order to reduce the effective flux of species collected by the sensor. Its potential is the same as the substrate i.e. 0V. A second grid polarized at -60V repels the electrons and lets the ions penetrate in the sensor. A third grid is used to discriminate the ion energy by sweeping its potential from -40 V up to 60 V. Finally, a last grid is used as collector to measure the effective ion current. By deriving the collected ion current over the sweeping potential we can then access the Ion Velocity Distribution

Function (IVDF) that is then plotted as a function of the retarding field. Finally, the total ion flux density is retrieved by integrating the IVDF and compensating the value by the transmission factor of the grids.

### B. Ion Flux Density Mapping

Each magnetic assembly is inserted in the cathode and the IVDF is measured for various position of the magnet with respect to the RFEA sensor that remains at a fixed position. We can thus access the normalized spatial distribution of the ion flux density that is presented in Fig. 5. The measures are taken at  $5 \cdot 10^{-3}$  mbar Kr pressure and 300 W plasma power.

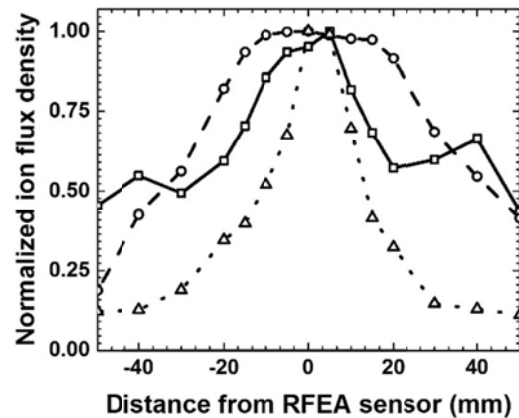


Fig. 5 Mapping of the ion flux density for balanced (open squares), unbalanced 1 (open circles) and unbalanced 2 (open triangles) configurations

One can notice a strong dependency of the ion flux density profile on the magnetic assembly. As expected the unbalanced configurations help to get a better control of the cavity area being bombarded with  $Kr^+$ . The unbalanced 2 configurations that exhibits the strongest unbalancing degree has a much directed ion flux which is focused on a 5 mm wide area compared to the unbalanced 1 which has a much more spread effect over the cavity surface.

In addition to the spatial distribution of the ion flux density one is interested in the absolute value of the ion flux density at the cavity surface.

### C. Ion Flux Density vs Discharge Power

The magnets are placed in the central position, facing the RFEA, and the ion flux density is measured with respect to the plasma power as reported in Fig. 6.

The unbalanced configurations clearly exhibit an increased ion flux density compared to the standard balanced configuration by a factor 1.7 and 4.6 for the unbalanced 1 and unbalanced 2, respectively.

Even though the improvement of ion flux on the surface matches our expectations it is interesting to look at the IVDF themselves as shown in Fig. 7. It appears that the increase in ion flux is obtained to the detriment of the ion energy. This can be understood by looking at the formula of the ions energy on a wall:

$$\varepsilon_i = \frac{eT_e}{2} \ln\left(\frac{M}{2.3m}\right) \sim 5.2eT_e \quad (2)$$

where  $\varepsilon_i$  is the ion energy in eV,  $T_e$  is the electron temperature in eV,  $M$  is the mass of the ions,  $m$  is the mass of the electron and  $e$  is the electron charge.

In the unbalanced configurations, the plasma is extended toward the cavity and then much more neutrals can be ionized. This induces a higher ion flux density, but in the same way more electrons participate to the ionization process and the average temperature of the electrons is reduced.

The only way to compensate this decrease in the ion energy and take all the benefit of the ion bombardment to assist the coating is to apply a bias voltage on the sample.

magnetron source. We have pointed out a drawback of the method that lies in the decrease of the ion energy at the surface of the sample, which will then have to be tuned by polarizing the sample. Next step will consist of fully characterizing the effect of such a plasma source on the quality of the deposited niobium film especially by focusing on the amount of voids in the layer and the potential improvement on tilted samples.

#### ACKNOWLEDGMENT

The work is part of EuCARD-2, partly funded by the European Commission, GA 312453

#### REFERENCES

- [1] C. Benvenuti, D. Boussard, S. Calatroni, E. Chiaveri, J. Tuckmantel, Production and test of 352 MHz Niobium sputtered reduced beta cavities, Proceedings of the 1997 Workshop on RF Superconductivity, 1038, 1997.
- [2] D. Tonini, C. Greggio, G. Keppel, F. Laviano, M. Musiani, G. Torzo and V. Palmieri, Morphology of niobium films sputtered at different target – substrate angle, proceedings of the 11<sup>th</sup> Workshop on RF Superconductivity, 614.
- [3] B Window and N. Savvides, J. Vac. Sci. Technol. A4(2), 196 (1986)
- [4] P.H. Mayrhofer, F. Kunc, J. Musil, C. Mitterer, A comparative study on reactive and non-reactive unbalanced magnetron sputter deposition of TiN coatings, vol. 415, 151-159 (2002).
- [5] D. C. Meeker, Finite Element Method Magnetics, Version 42 (12Jan2016 Build), <http://www.femm.info>
- [6] I.V. Svadkovski, D.A. Golosov and S.M. Zavatskiy. Characterisation parameters for unbalanced magnetron sputtering systems, Vacuum, 68, pp. 283–290, 2003.

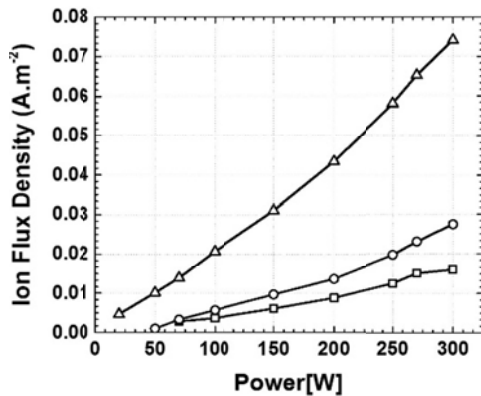


Fig. 6 Ion flux density at the cavity surface versus discharge power for balanced (open squares), unbalanced 1 (open circles) and unbalanced 2 (open triangles) configurations

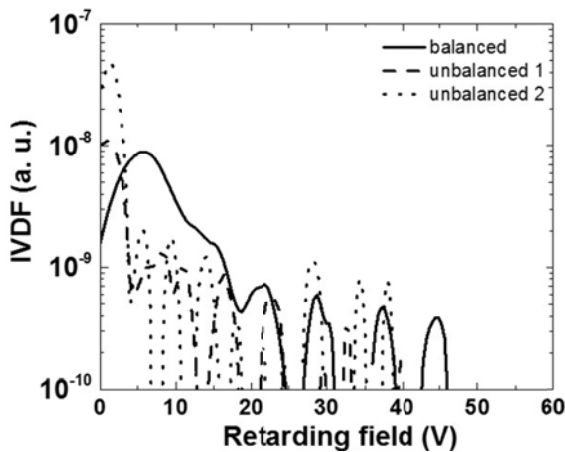


Fig. 7 IVDF for the three different magnetic configurations at a pressure of  $5 \cdot 10^{-3}$  mbar and 300W of discharge power

#### VI. CONCLUSION AND PERSPECTIVES

In order to improve the thin film properties in SRF cavities we have proposed a technical solution to fabricate an unbalanced plasma source in a cylindrical geometry. The magnetic properties of the source have been simulated and confirmed by mean of magnetic probe measurements. Furthermore, we have qualified the gain in ion flux density using such a source compared to a traditional balanced